Computational and Structural Biotechnology Journal 20 (2022) 485–495

COMPUTATIONAL AND STRUCTURAL BIOTECHNOLOGY JOURNAL

journal homepage: www.elsevier.com/locate/csbj

# Comparative metabolomics revealed key pathways associated with the synergistic killing of multidrug-resistant *Klebsiella pneumoniae* by a bacteriophage-polymyxin combination

Mei-Ling Han [a,*], Sue C. Nang [a], Yu-Wei Lin [a], Yan Zhu [a], Heidi H. Yu [a], Hasini Wickremasinghe [a], Christopher K. Barlow [b,c], Darren J. Creek [c,d], Simon Crawford [e], Gauri Rao [f], Chongshan Dai [g], Jeremy J. Barr [h], Kim Chan [i], Robert Turner Schooley [j], Tony Velkov [k], Jian Li [a,*]

[a] *Biomedicine Discovery Institute, Infection and Immunity Program, Department of Microbiology, Monash University, Clayton, Victoria 3800, Australia*
[b] *Department of Biochemistry and Molecular Biology, Monash University, Clayton, VIC, Australia*
[c] *Monash Proteomics and Metabolomics Facility, Monash Biomedicine Discovery Institute, Monash University, Clayton, Victoria 3800, Australia*
[d] *Drug Delivery, Disposition and Dynamics, Monash Institute of Pharmaceutical Sciences, Monash University, 381 Royal Parade, Parkville, Victoria 3052, Australia*
[e] *Ramaciotti Centre for Cryo Electron Microscopy, Monash University, Australia*
[f] *Division of Pharmacotherapy and Experimental Therapeutics, Eshelman School of Pharmacy, University of North Carolina, Chapel Hill, NC 27599, USA*
[g] *Department of Veterinary Pharmacology and Toxicology, College of Veterinary Medicine, China Agricultural University, No.2 Yuanmingyuan West Road, Beijing 100193, China*
[h] *School of Biological Sciences, Monash University, 25 Rainforest Walk, Clayton, Victoria 3800, Australia*
[i] *Advanced Drug Delivery Group, School of Pharmacy, Faculty of Medicine and Health, The University of Sydney, Sydney, NSW 2006, Australia*
[j] *Division of Infectious Diseases and Global Public Health, Department of Medicine, University of California San Diego, La Jolla, CA, USA*
[k] *Department of Pharmacology & Therapeutics, School of Biomedical Sciences, Faculty of Medicine, Dentistry and Health Sciences, The University of Melbourne, Parkville, Victoria 3010, Australia*

ARTICLE INFO

*Article history:*
Received 26 September 2021
Received in revised form 28 December 2021
Accepted 30 December 2021
Available online 06 January 2022

*Keywords:*
*Klebsiella pneumoniae*
Polymyxin resistance
Bacteriophage
Metabolome
Central carbon metabolism

ABSTRACT

Resistance to the last-line polymyxins is emerging in multidrug-resistant *Klebsiella pneumoniae* and phage therapy is a promising alternative. However, phage monotherapy often rapidly causes resistance and few studies have examined antibiotic-phage combinations against *K. pneumoniae*. Here, we investigated the combination of polymyxin B with a novel phage pK8 against an *mcr*-1-carrying polymyxin-resistant clinical isolate Kp II-503 (polymyxin B MIC, 8 mg/L). The phage genome was sequenced and bacterial metabolomes were analysed at 4 and 24 h following the treatment with polymyxin B (16 mg/L), phage pK8 ($10^2$ PFU/mL) and their combination. Minimal metabolic changes across 24 h were observed with polymyxin B alone; whereas a significant inhibition of the citrate cycle, pentose phosphate pathway, amino acid and nucleotide metabolism occurred with the phage-polymyxin combination at both 4 and 24 h, but with phage alone only at 4 h. The development of resistance to phage alone was associated with enhanced membrane lipid and decreased amino acid biosynthesis in Kp II-503. Notably, cAMP, cGMP and cCMP were significantly enriched (3.1–6.6 $\log_2$fold) by phage alone and the combination only at 4 h. This is the first systems pharmacology study to investigate the enhanced bacterial killing by polymyxin-phage combination and provides important mechanistic information on phage killing, resistance and antibiotic-phage combination in *K. pneumoniae*.



## 1. Introduction

*Klebsiella pneumoniae* is a nosocomial pathogen that can cause chronic and acute respiratory and bloodstream infections [1,2]. Multidrug-resistant (MDR) *K. pneumoniae* is particularly difficult to treat as it possesses a high level of intrinsic and adaptive resistance to almost all antibiotics [3]. Polymyxins (i.e. polymyxin B and colistin) are often the only available therapeutic option for MDR *K. pneumoniae* [4,5]. Polymyxins are a class of cyclic lipopeptides that are mainly active against Gram-negative bacteria due to their unique antibacterial mechanism. Worryingly, hospital- and community-acquired infections caused by polymyxin-resistant MDR *K. pneumoniae* have been increasingly reported over the past decade [6–8]. Resistance to polymyxins significantly threatens our

* Corresponding authors.
*E-mail addresses:* meiling.han@monash.edu (M.-L. Han), jian.li@monash.edu (J. Li).

https://doi.org/10.1016/j.csbj.2021.12.039

antibiotic armamentarium for the treatment of MDR Gram-negative organisms, including *K. pneumoniae*.

As the development of new antibiotics to combat emerging resistance has stagnated over the last two decades, bacteriophage (phage) therapy has garnered renewed attentions as an approach to treat MDR bacterial infections [9,10]. Regulations and policy on the clinical use of phages are now revisited by Western countries, opening a new avenue for the treatment of MDR bacterial infections [11,12]. Compared to antibiotics, phage therapy is typically safe, has a much narrower antibacterial spectrum, and can be effective against both antibiotic-susceptible and -resistant bacteria [13,14]. However, as with antibiotic therapy, a notable limitation for phage therapy is that bacteria can rapidly evolve resistance to phages [9]. Furthermore, the narrow antibacterial spectrum of phage therapy is very challenging in the clinic and requires rapid diagnosis. Given this situation, the combination of a phage and antibiotic(s) may provide a superior strategy for controlling bacterial pathogens than phage monotherapy [15]. Compared to each monotherapy, bacteria-phage combinations can enhance antibacterial killing, reduce incidence of resistance to both the antibiotic and phage, and lower host toxicities [16–20]. As the propagation of phages depends on bacterial metabolism [9,21], it is critical to understand the impact of antibiotic, phage and synergistic antibiotic-phage combination on bacterial metabolism and resistance in order to optimise their clinical use. Currently, very few of antibiotic-phage combination studies examined the activity against pandrug-resistant *K. pneumoniae* [15,22–24]. Polymyxins disorganise the outer membrane and kill bacteria eventually, while phages propagate within bacteria and lyse cells [25]. Furthermore, in their unique antibacterial activities both polymyxins and phages substantially perturb bacterial metabolism [25,26]. In the present study, we discovered synergistic killing of a novel phage in combination with the polymyxin against a polymyxin-resistant MDR clinical isolate *K. pneumoniae* II-503. This bacterial strain contains the plasmid-borne phosphoethanolamine (pEtN) transferase gene *mcr-1* which has generated significant concerns of potential rapid dissemination of resistance to the last-line polymyxins via horizontal transfer worldwide [27]. Notably, significant inhibition of the citrate cycle, pentose phosphate pathway, amino acid and nucleotide metabolism was revealed with the polymyxin-phage combination.

## 2. Material and methods

### 2.1. Chemical and reagents

Polymyxin B (sulphate) was obtained from Beta Pharma (Shanghai, China). Stock solutions (5 mg/mL) were prepared using Milli-Q water and filtered through 0.22-μM syringe filters (Sartorius, Melbourne, VIC, Australia). All organic solvents (chloroform, methanol and acetonitrile) used in metabolite extraction and liquid chromatography-mass spectrometry (LC-MS) were LC-MS grade and purchased from Merck Millipore (Bayswater, VIC, Australia).

### 2.2. Bacterial isolates and the isolation and purification of bacteriophages

A clinical isolate *K. pneumoniae* II-503 was collected from a urine sample of a hospitalised patient (Zhejiang, China) [27] and employed in this study. The minimum inhibitory concentration (MIC) of polymyxin B against *K. pneumoniae* II-503 (8 mg/L) was measured with a broth microdilution method [28]. Prior to each experiment, *K. pneumoniae* II-503 was subcultured on Mueller-Hinton agar and incubated at 37 °C for approximately 18 h. Single colonies were then inoculated into 20 mL of Luria-Bertani (LB) broth for 16–18 h in a shaking water bath (180 rpm, 37 °C). The Phage On Tap (PoT) protocol was used for the isolation, purification and amplification of bacteriophage pK8 [29]. Briefly, 10 mL of raw sewage sample was added to an equal volume of the above bacterial overnight culture, followed by a further 1:10 dilution with sterile LB broth. The sewage-bacteria-phage culture was incubated for 24 h at 37 °C in a shaking water bath (200 rpm) and then centrifuged at 3,200 × *g* for 10 min at 4 °C to collect phage in the supernatant. After filtration through a 0.22-μM filter, the raw phage lysate was spotted onto a double-layer plate containing bacterial culture in the top layer and nutrient agar in the bottom layer. After 24-h incubation, the plaque assay and overlay methods were used to isolate new phages [29]. A new phage was then purified and propagated for the studies below. The methods including scanning electron microscopy, flow cytometry and phage whole genome sequencing were described in the Supplementary Information.

### 2.3. Static time-kill kinetics of polymyxin B, phage pK8 and their combination against K. pneumoniae II-503

To optimise the phage-polymyxin combination and determine the optimal condition for the metabolomics study below, the time-kill kinetics of phage pK8 at different multiplicities of infection (MOI) were firstly examined. Briefly, overnight culture of *K. pneumoniae* II-503 (200 μL) was incubated in 20 mL CAMHB for 2 h at 37 °C, and then diluted at 1:100 with CAMHB to obtain a starting inoculum of approximately $10^6$ CFU/mL. This culture was treated with phage pK8 at $10^6$, $10^5$, $10^4$, $10^3$, $10^2$, 10 PFU/mL for 1, 2, 3, 4, 6 and 24 h; 1 mL sample at each time point was collected for phage and bacterial enumeration. The samples were centrifuged at 10,000*g* for 10 min at 4 °C and the supernatant was collected for phage quantification while the cell pellet for bacterial viable counting. The phage was quantified using plaque assay [30]. Briefly, 100 μL of *K. pneumoniae* II-503 ($10^6$ CFU/mL) and 100 μL of the serially diluted phage sample from the above supernatant were added into a sterile glass tube, vortexed and left at room temperature for 10 min. The sample was then mixed with 3 mL of 0.5% soft agar, poured onto a nutrient agar plate, and finally incubated at 37 °C for overnight. Similarly, the time-kill kinetics of polymyxin B (16 mg/L), phage pK8 ($10^2$ PFU/mL) and their combination against *K. pneumoniae* II-503 was also conducted and bacterial cell pellets were collected at 1, 4 and 24 h under each condition for bacterial viable counting. Bacterial colonies (n = 3) of the treated samples and untreated control were randomly selected to examine resistance to the phage (plaque assay as mentioned above) and polymyxin B (MIC measurement with broth microdilution) [28,31].

### 2.4. Metabolite extraction for the metabolomics experiment

In the metabolomics experiment, 4 h was examined for the rapid bacterial killing by both the phage and polymyxin B (as the representative of polymyxins considering their very similar structures and pharmacological characteristics [25]); while 24 h was employed to examine the persistent antibacterial effect and potential emergence of resistance to the phage and polymyxin B. At 0, 4 and 24 h, 20 mL of the above bacterial culture ($n = 4$) was collected and immediately quenched in a dry ice-ethanol bath to stop metabolic processes. Normalised bacterial samples (10 mL at $OD_{600}$ = 0.50 ± 0.02) were centrifuged at 3200*g* for 10 min at 4 °C and the supernatant was removed. Bacterial cell pellets were washed twice with ice-cold 0.9% saline and resuspended in 0.5 mL of chloroform/methanol/water (1:3:1, v/v) extraction solvent which contained 1 μM internal standards (CHAPS, CAPS, PIPES and TRIS) to assess the extraction efficiency. Bacterial suspension was frozen in liquid

nitrogen and thawed in ice for three times to ensure bacterial lysis and metabolite extraction. Samples were then centrifuged at 3200*g* and 4 °C for 10 min to remove cell debris, and particle-free supernatant was obtained by further centrifugation at 14,000*g* and 4 °C for 10 min for LC-MS analysis.

### 2.5. Metabolic profiling using liquid chromatography-mass spectrometry

The above metabolite samples were analysed on a Dionex U3000 high-performance liquid chromatography (HPLC) system in tandem with a Q-Exactive Orbitrap high-resolution mass spectrometer (Thermo Fisher) in both positive and negative mode with a mass range of 85–1275 *m/z*. A previously described hydrophilic interaction liquid chromatography (HILIC) method was employed [32]. Briefly, samples (10 μL, maintained at 6 °C) were eluted through a ZIC-pHILIC column (5 μm, polymeric, 150 × 4.6 mm; SeQuant, Merck) by mobile phases containing 20 mM ammonium carbonate in lane A and acetonitrile in lane B (flow rate, 0.3 mL/min). A linear gradient from 80% mobile phase B to 50% of mobile phase B was employed over the first 15 min, then to 5% mobile phase B at 18 min, and followed by a washing step containing 5% mobile phase B for 3 min. An 8-min re-equilibration step with 80% mobile phase B was conducted prior to the next injection. All samples were analysed within the same LC-MS batch to minimise analytical variations. A pooled quality control sample consisting of 10 μL of each sample was analysed periodically throughout the batch to assess chromatographic peaks, signal reproducibility and analyte stability. A total of 8 external standard samples containing a mixture of >300 authentic standards were also analysed within the batch to assist metabolite identification.

### 2.6. Data processing, statistical analysis and metabolic pathway mapping

Untargeted metabolomics data analysis was performed in IDEOM version 20 workflow [33]. Briefly, this involved mass peak picking with XCMS [34], peak alignment and filtering with mzMatch [35], and further filtering, metabolite annotation, and comparative analysis with IDEOM. Metabolites were identified based on accurate mass (<2 ppm) and retention time (<50%). Metabolites that matched to authentic standards were considered as level 1 identifications, while other putative metabolites based on accurate mass and predicted retention time were deemed level 2 annotations [36]. Statistical analysis including one-way analysis of variance (ANOVA), principal component analysis (PCA) was performed in MS Excel, R and Metaboanalyst 4.0 [37]. Prior to statistical analysis, metabolomics data were normalised to the median height of all putatively identified peaks and $\log_2$-transformed. The *p* value obtained from ANOVA was corrected based on Benjamini-Hochberg correction and the group difference assessed by Post-Hoc analysis (Fisher's least significant difference) [38]. Metabolites showing ≥2-fold change (adjusted $p < 0.05$) were further analysed for pathway analysis using KEGG (Kyoto Encyclopedia of Genes and Genomes) and Ecocyc pathways with reference to *Escherichia coli* K-12 MG1655.

## 3. Results

### 3.1. Time-kill kinetics and bacterial phenotypical changes following treatment with polymyxin B monotherapy, phage pK8 monotherapy, and their combination

Phage pK8 at different multiplicities of infection (MOI) produced a maximal initial killing of 6–8 $\log_{10}$ CFU/mL at 1–4 h, followed by substantial regrowth such that bacterial numbers had increased close to the control values at 24 h (Fig. 1A). Regardless the MOIs ($10^{-6}$ to 1), the greatest killing was observed with the phage density reaching to $>10^8$ PFU/mL (Fig. 1B). When in combination with polymyxin B (16 mg/L), the bacterial killing was remarkably enhanced compared to each treatment alone (Fig. 1C); while polymyxin B only slightly affected the replication of phages across 24 h (Fig. 1D). Furthermore, bacterial regrowth to the control levels was only observed at 24 h with both monotherapies after an initial killing of 1-$\log_{10}$ CFU/mL by polymyxin B alone and 5–6 $\log_{10}$ CFU/mL by phage alone at 4 h. Despite the slightly reduced phage number in the polymyxin-phage combination compared to phage alone, the combination caused much better bacterial killing and minimised bacterial regrowth across 24 h (Fig. 1C and D). Importantly, randomly selected bacterial colonies treated with phage alone for 24 h showed phage resistance, which was largely minimised by the combination (Fig. S1). Importantly, phage-resistant bacterial cells in the phage alone group displayed similar polymyxin susceptibility as the control (i.e. untreated bacteria). Our SEM imaging showed lysed cells with phage pK8 alone ($10^2$ PFU/mL, i.e. $10^{-6}$ MOI) (Fig. 1E); whereas both polymyxin B alone (16 mg/L) and the polymyxin B-phage pK8 combination induced vesicles and long-tube like structures on the cell surface at 4 h, but only vesicles were observed at 24 h (Fig. 1E). At both time points, lysed cells were present with the polymyxin B-phage pK8 combination, but not observed with phage monotherapy at 24 h, which confirmed resistance to phage alone and the synergistic killing by the combination (Fig. 1E). Unlike the treatment of phage pK8 alone, both polymyxin B alone and the polymyxin B-phage combination caused significant membrane depolarisation over 24 h; in particular, the entire bacterial population treated with the combination showed decreased membrane potential at 24 h (Fig. S2).

### 3.2. Genomic analysis of phage pK8

The novel phage pK8 [GenBank accession number: OL702938] consisted of a circular genome of 49,534 bp with a G + C content of 51.1%. A total of 77 protein-coding genes were identified with the majority ($n$ = 48) of hypothetical function; whereas 12 genes were identified that were associated with DNA transit and replication, 2 with DNA packaging, 12 with morphogenesis (tail fibre [$n$ = 10] and head [$n$ = 2]), and 3 with lytic functions (Supplementary dataset 1). Notably, no integrase gene was identified in the genome of pK8. BLAST analyses of the pK8 genome sequence revealed a significant similarity (coverage, 96–98%; identity, 95–98%) to eight *K. pneumoniae* phages (PhiKpNIH-10 [MN395285.1], vB_KpnS_15-38_KLPPOU149 [MN689779.1], GML-KpCol1 [MG552615.1], MezzoGao [MF612072.1], NJR15 [MH633487.1], KPN N141 [MF415412.1], KpKT21phi1 [MK278861.1] and Sweeny [MK931443.1]). Multiple alignment revealed that phage pK8 was highly similar to phages PhiKpNIH-10, vB_KpnS_15-38_KLPPOU149, GML-KpCol1 and MezzoGao, with several variations in the genes encoding hypothetical proteins (Fig. 2). Notably, despite the many similarities, among the known functional protein-coding genes, a gene encoding a tail fibre protein in pK8 showed differences in the nucleotide sequence when compared to the same gene in the remaining four highly similar phages: Sweeny (coverage 100%; identity 87%), NJR15 (coverage 76%; identity 95%), KPN N141 (coverage 67%; identity 90%) and KpKT21phi1 (coverage 49%; identity 85%).

### 3.3. Global metabolic variations in response to phage and polymyxin B alone and the combination

According to the principal component analysis (PCA) score plots in our metabolomics study (Fig. 3A), the metabolic perturbations caused by phage pK8 alone and in combination with polymyxin B

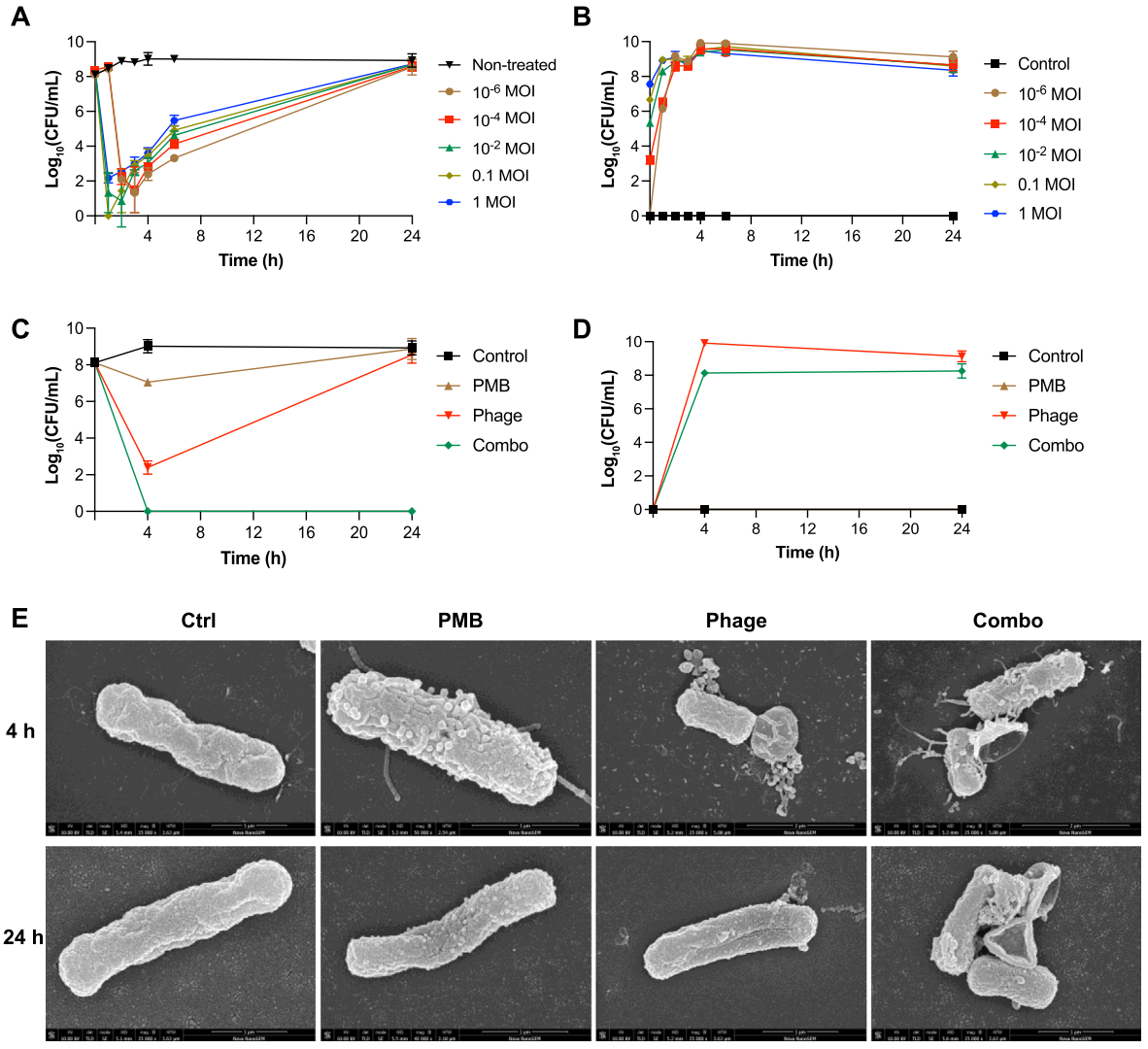


**Fig. 1.** (A) Time-kill kinetics of *K. pneumoniae* II-503 following the treatments with phage pK8 at different multiplicities of infection (MOI); (B) Growth kinetics of phage pK8 following the infection of *K. pneumoniae* II-503 with different MOIs; (C) Time-kill kinetics of *K. pneumoniae* II-503 following treatments with polymyxin B alone (PMB; 16 mg/L, 2 × MIC), phage pK8 alone ($10^2$ PFU/mL, $10^{-6}$ MOI), and the combination (Combo); untreated control (Ctrl) was included; and (D) Phage growth kinetics when infecting *K. pneumoniae* II-503 in the absence or presence of polymyxin B; $n = 3$. (E) Representative scanning electron microscopy (SEM) images at 4 and 24 h of *K. pneumoniae* II-503 cells receiving no treatment (control; Ctrl) or treatment with polymyxin B (PMB; 16 mg/L) alone, phage ($10^2$ PFU/mL) alone, and the combination (Combo).

at 4 h were significantly different compared to those observed with polymyxin B alone and the untreated control (PC1 = 76.3%). In contrast, at 24 h the PCA plot is dominated by the separation of the combination samples from all other samples along PC1 (84.9%). Moreover, through PCA analysis of all the sample groups at both 4 and 24 h, the metabolomic profiles of the combination samples at 24 h closely represent that of the phage alone and combination samples at 4 h. In total, the number of significantly affected metabolites at 4 h was 44/74 (up/down), 184/325, and 196/350 following treatment with polymyxin B, phage pK8, and the combination, respectively ($\log_2$ fold change $\geq 1$ or $\leq -1$, adjusted $p$-value <0.05, ANOVA; Fig. 3B, Supplementary dataset 2). The corresponding values at 24 h were 12/5, 40/18, and 202/416 (Fig. 3B). Notably, at 4 h there were 103 metabolites commonly affected by all three treatments (Fig. 3B). These metabolites are involved in central carbon metabolism (e.g. coenzyme A, citrate, 3-phospho-D-glycerate, D-sedoheptulose 7-phosphate), lysine (e.g. *N*-acetyl-L-lysine and diaminoheptanedioate) and arginine (e.g. glutamate, ornithine and *N*-acetyl-ornithine) biosynthesis, glutathione metabolism (e.g. glutathione disulfide), purine (e.g. GMP, GDP and GTP) and pyrimidine (e.g. cytosine, cytidine, CMP, CDP and CTP) metabolism, as well as phospholipids [e.g. PA(33:1), PE(34:1), lysoPE(18:1), PG (32:1), lysoPG(18:1) and CL(68:3)] (Fig. 4A). At 4 h, the metabolite levels associated with amino acid, carbohydrate and nucleotide metabolism were significantly decreased with phage pK8 alone and the combination, whereas metabolites associated with fatty acid and phospholipid metabolism were significantly enriched (Fig. 3C). Although phage alone did not significantly affect bacterial metabolism at 24 h, significant perturbations in carbohydrate, lipid, amino acid and nucleotide metabolism remained at this time with the combination (Fig. 3C). Interestingly, the metabolic changes in amino acid (e.g. L-ornithine and glutathione disulfide) and central carbon (e.g. D-glyceraldehyde 3-phosphate, D-fructose 6-phosphate, and D-sedoheptulose 1,7-biphosphate) metabolism caused by phage monotherapy at 24 h were in the opposite direction than were observed at 4 h (Fig. 4B).

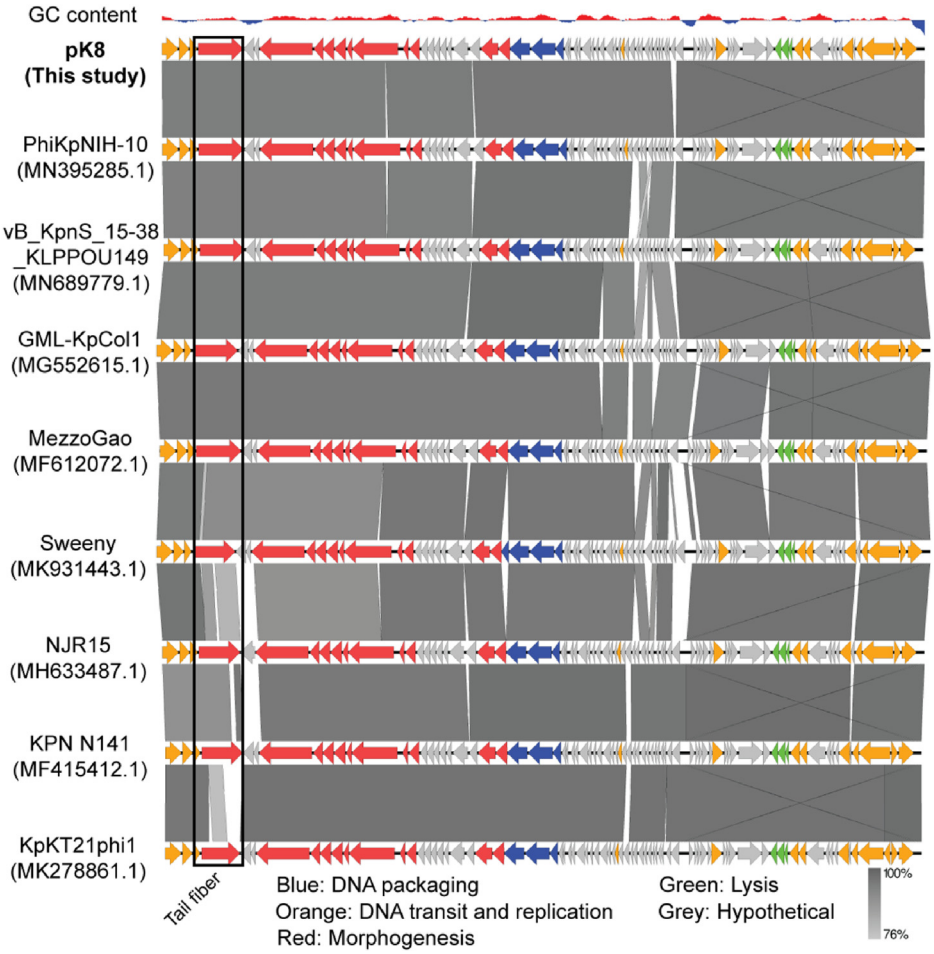


**Fig. 2.** Multiple alignment of the genomes of phage pK8 and eight *K. pneumoniae* phages available in GenBank.

### *3.4. The pentose phosphate pathway and citrate cycle were drastically inhibited by phage alone and the polymyxin B-phage combination*

Our data showed that phage alone and its combination with polymyxin B perturbed a number of metabolites related to central carbon metabolism at 4 h; however, only the combination showed significant differences at 24 h. Specifically, the levels of five key metabolites (6-phospho-D-glucono-1,5-lactone, D-gluconate 6-phosphate, D-sedoheptulose 7-phosphate, D-fructose 6-phosphate and D-glucono-1,5-lactone) in pentose phosphate pathway (PPP) were significantly decreased by phage alone and the combination at 4 h ($\log_2$FC > 1, FDR < 0.05; Fig. 5A); whereas, these metabolites (except D-glucono-1,5-lactone) remained significantly decreased at 24 h only with the combination ($\log_2$FC < −1, FDR < 0.05; Fig. 5A). Interestingly, the level of D-gluconate ($\log_2$FC = 1.4–2.6) increased with both phage alone and the combination at 4 h, indicating that the conversion of D-gluconate to D-gluconate 6-phosphate was inhibited. Both treatments at 4 h, but only the combination therapy at 24 h, also greatly inhibited the citrate cycle and significantly depleted all the identified metabolites associated with this pathway ($\log_2$FC < −1, FDR < 0.05; Fig. 5B). Moreover, although polymyxin B alone at 16 mg/L did not significantly affect the central carbon metabolism over 24 h, the relative abundance of CoA and citrate was significantly reduced at 4 h.

In contrast to the combination, phage alone induced unique changes in central carbon metabolism at 24 h. As precursors involved in bacterial lipid and cell wall synthesis, the levels of D-glyceraldehyde 3-phosphate ($\log_2$FC = 1.3), D-sedoheptulose 1,7-biphosphate ($\log_2$FC = 2.6) and D-fructose 6-phosphate ($\log_2$FC = 1.6), were significantly increased with phage alone at 24 h (Fig. 4B). Conversely, the levels of phosphoenolpyruvate ($\log_2$FC = −1.4) and glycerate 3-phosphate ($\log_2$FC = −1.5) which were both involved in the synthesis of Tyr, Trp, Cys, Gly and Ser, were greatly decreased by phage alone at 24 h (Fig. 4B).

### *3.5. Amino acid and nucleotide metabolism was significantly disturbed by phage alone and the combination*

With phage alone, the increased abundance in a number of amino acids at 4 h (i.e. His, Pro, and Thr) and 24 h (i.e. Glu, His and Lys) was observed, with similar increases observed with the combination (i.e. His, Phe, Pro, Thr, Try and Tyr at 4 h; and Pro and Thr at 24 h) ($\log_2$FC > 1, FDR < 0.05; Fig. 6A). Decreased levels in Asn, Glu, Gln, Lys, Ser and Val were observed with phage alone at 4 h and the combination at 4 and 24 h ($\log_2$FC < −1, FDR < 0.05). The nucleotide metabolism was also significantly affected, with the phosphorylated nucleotides and their free bases significantly reduced by all three treatments at 4 h, but only by the combination at 24 h (Fig. 6B). Interestingly, three cyclic nucleotides (2′,3′-cyclic AMP, 3′,5′-cyclic GMP, and 2′,3′-cyclic CMP) likely related to cellular messaging were significantly enriched ($\log_2$FC = 3.1–6.6) by phage alone and the combination only at 4 h (Fig. 6C). Moreover, glutathione (GSH) and glutathione disulphide (GSSG) were significantly decreased by all three treatments at 4 h and only the combination at 24 h ($\log_2$FC < −1, FDR < 0.05; Fig. 6D); whereas both were increased by phage alone at 24 h (GSH $\log_2$FC = 0.95 and

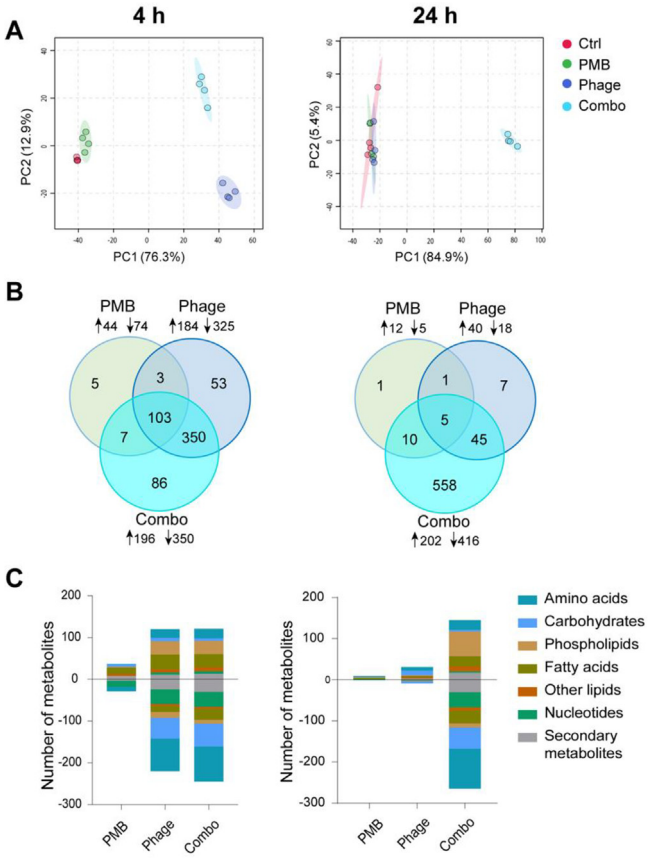


**Fig. 3.** Multivariate and univariate statistical analysis of global metabolic changes at 4 h (left) and 24 h (right). (A) PCA score plots of the first two principal components for metabolite levels in *K. pneumoniae* II-503 following no treatment (Ctrl) or treatment with polymyxin B (PMB) alone, phage pK8 alone, and their combination (Combo). A total of 16 samples with 4 biological replicates under each condition are displayed in each dataset. (B) Venn diagrams showing the number of significantly affected metabolites with each treatment. (C) Bar charts showing the number of significantly affected metabolites in each main class with each treatment. Positive and negative values indicate the number of significant metabolites whose intracellular levels were increased and decreased, respectively. Significant metabolites were selected based on $|\log_2 FC| \geq 1$ with adjusted *p*-value <0.05 (one-way ANOVA, Benjamini-Hochberg correction).

GSSG $\log_2$FC = 1.4; Figs. 3B and 6D). Significant reductions of reduced nicotinamide adenine dinucleotide (NADH), flavin mononucleotide (FMN), and flavin adenine dinucleotide (FAD) were consistently observed with phage alone and combination at 4 h while only with the combination at 24 h (Fig. 6E).

### 3.6. Lipid levels were significantly perturbed by all three treatments

All three treatments significantly affected bacterial lipid levels at both 4 and 24 h. The levels of fatty acids were generally increased with phage monotherapy (at 4 h) and the combination (at 4 and 24 h; Fig. 4); however, the metabolic changes in bacterial membrane phospholipids were class-dependent (Fig. 7). At 4 h, all treatments substantially increased the levels of phosphatidic acids [PA, e.g. PA(26:1), PA(27:1) and PA(33:1)], phosphatidylethanolamine [PE, e.g. PE(32:1) and PE(34:1)], cardiolipin [CL(68:3)] and phosphatidylserine [PS, e.g. PS(52:0)]; whereas the levels of lysoPE [e.g. lysoPE(16:0), lysoPE(17:1) and lysoPE (18:0)] and lysophosphatidylglycerol [lysoPG(18:1)] were only significantly increased with phage alone and the combination. However, there was a dramatic reduction in the levels of PG [e.g. PG (30:0), PG(33:1), PG(34:1) and PG(35:1)] with the combination at 4 h, with a much smaller reduction observed with phage alone at this time (Fig. 7A). Notably, with the exception of several PE species [e.g. PE(29:0), PE(32:4) and PE(35:5)] which were decreased at 24 h compared to 4 h (Fig. 7B), the combination induced similar changes in phospholipid levels at both 4 and 24 h.

## 4. Discussion

With the increasing resistance to almost all current antibiotics, including the last-line polymyxins [39,40], novel treatments are urgently required for Gram-negative 'superbugs', in particular MDR *K. pneumoniae*. Therefore, phage therapy has emerged as a promising option, in particular when synergistically combined with antibiotics [17]. Unfortunately, the current literature on antibiotic-phage combinations against *K. pneumoniae* is scarce. The present study is the first to use systems pharmacology to investigate the synergistic bacterial killing of a phage-antibiotic combination against *K. pneumoniae*.

Our genomic analysis revealed no integrase gene in the genome of pK8, demonstrating that it is very likely a highly virulent phage; this is confirmed by the rapid killing kinetics against an *mcr*-carrying polymyxin-resistant clinical isolate *K. pneumoniae* II-503 (Fig. 1A). Phage pK8 shares similarities with eight other *K. pneumoniae* phages available in GenBank. The most distinct finding from the comparative analysis of these phages was a low sequence identity in a gene encoding for a tail fibre protein. Given the key role of tail fibres in the specific recognition of bacterial surface during the initial step of viral infection [41,42], the notable difference between pK8 and four other highly similar phages (NJR15, KPN N141, KpKT21phi1 and Sweeny) in the nucleotide sequence suggests that pK8 may target a different receptor on bacterial surface.

We have shown that the combination of polymyxin B with phage pK8 significantly enhanced bacterial killing and minimised phage resistance of a polymyxin-resistant, MDR clinical isolate of *K. pneumoniae* (Fig. 1C and S1). Indeed, while both phage pK8 alone and polymyxin B-phage pK8 combination produced substantial initial killing, the reduced bacterial regrowth (~8 $\log_{10}$ CFU/mL) was only observed with the combination at 24 h, whereas bacterial regrowth with phage alone had reached the level of the control (~9 $\log_{10}$ CFU/mL). A high starting inoculum (~$10^8$ CFU/mL) was used for the metabolomics experiments to ensure the responses observed were due to antibiotic and/or phage treatments but not extensive bacterial killing. Two time points 4 and 24 h were selected to investigate the antibacterial effect of phages on polymyxin-resistant *K. pneumoniae* in the presence of polymyxins which display initial bactericidal killing but often regrowth afterwards [43].

Our results revealed distinct differences in cell surface morphology and membrane potential of *K. pneumoniae* following the treatment with polymyxin B, phage pK8, or the combination (Fig. 1E and S2). These differences are primarily due to phage-induced lytic cell death necessary for the release of phage progeny [44], whereas the antimicrobial activity of the polymyxins is exerted mainly through disruption of the bacterial outer membrane [45]. Our SEM imaging demonstrated that polymyxin B treatment produced vesicles on the cell surface of *K. pneumoniae* II-503, as has been shown previously in *Escherichia coli* and *Pseudomonas aeruginosa* [46,47]. Outer membrane vesicles are thought to have an important role in the immediate bacterial defence against stressors targeting the cell envelope, including antibiotics [46]. The increase in vesiculation demonstrated that polymyxin B was still able to disorganise the OM of resistant *K. pneumoniae* II-503 even without killing. Bacterial vesiculation has been shown to decrease the infectivity of bacteriophage T4 in *E coli* [46], although decreased infectivity was not observed in the current

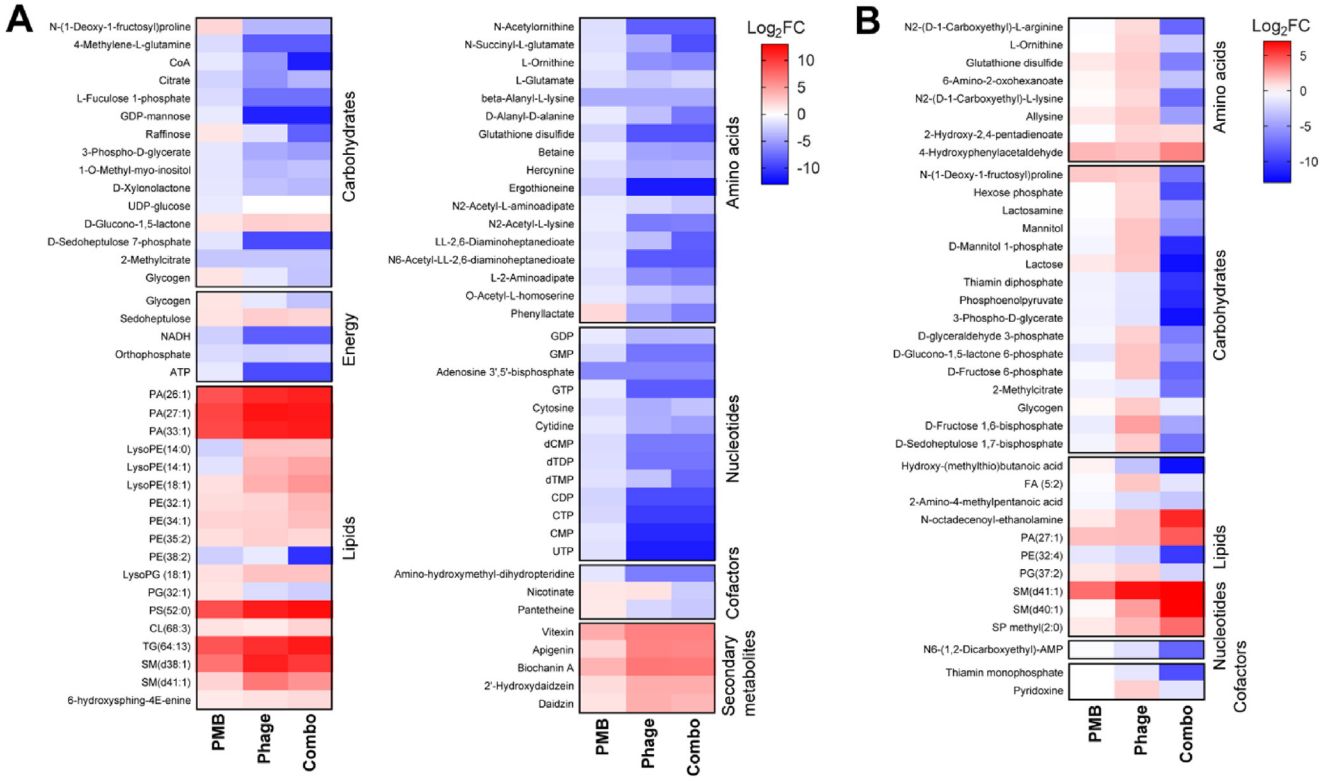


**Fig. 4.** (A) Heatmap profiles at 4 h showing the commonly affected metabolites associated with all three treatments (polymyxin B [PMB] alone, phage pK8 alone, and the combination [Combo]); (B) Heatmap profiles at 24 h showing the commonly affected metabolites associated with polymyxin B (PMB) alone, phage pK8 alone and the combination. Metabolites are grouped into different classes: carbohydrates, lipids, amino acids, nucleotides, co-factors, secondary and energy metabolites. The colours indicate the $\log_2$ fold changes (FC) of significant metabolites associated with the different treatments compared to the untreated control at each time point. Blue, decrease; red, increase. (For interpretation of the references to colour in this figure legend, the reader is referred to the web version of this article.)

study with our phage pK8. Interestingly, the polymyxin B-phage combination resulted in a mixture of lysed cells and cells with surface vesicles, suggesting a level of separate activities by each treatment (i.e. lysis induced by the phage and membrane disruption by polymyxin B); importantly, antibacterial activity was markedly improved with the combination (Fig. 1).

Our metabolomics data showed that the significant metabolic perturbations by the combination of phage pK8 and polymyxin B were very similar between 4 and 24 h, which were similar with phage alone only at 4 h but not at 24 h due to the rapid emergence of resistance (Figs. 4–6). This indicated that the synergy of this combination at 4 h was mainly driven by phage pK8, while resistance to the phage or antibiotic alone was prevented at 24 h. The enhanced bacterial killing of the polymyxin-phage combination involved significant metabolic alterations in the citrate cycle, pentose phosphate pathway, amino acid and nucleotide metabolism, as well as membrane lipid synthesis. Both the citrate cycle and PPP are essential pathways of central carbon metabolism that generate energy and precursors for synthesising the biomass of bacterial cells [48,49]. The dramatic depletion of central carbon metabolism directly resulted in significant perturbations of amino acid and nucleotide metabolism, as well as reductions in energy (e.g. ADP and ATP) and redox (e.g. NADH) related metabolites, indicating a shutdown of bacterial metabolism (Fig. 6). These findings were also observed with the combination across 24 h, which led to the inhibition of bacterial regrowth (Fig. 5). A similar depletion by phage alone was only observed at 4 h, with several unique metabolic changes possibly related to phage resistance at 24 h as discussed below.

Phages rely on the metabolism of the host bacterial cell to complete their infection process, and bacterial nucleotides and amino acids are essential for phage genome replication and successful completion of its infection cycle [21,26,50,51]. Differential changes were observed in the levels of different amino acids at both time points, suggesting uneven utilisation by the phage. For example, the intracellular levels of Asn and Lys were significantly decreased by phage alone at 4 h, while His, Pro and Thr substantially increased (Fig. 6A). In general, at 4 h the combination caused similar perturbations in amino acid metabolism as by phage alone (Fig. 6A), indicating the metabolic change at this time was dominated by the phage. Whereas at 24 h the combination caused significant alterations in amino acid metabolism relatively similar to at 4 h but with higher fold changes, including reductions in the levels of most amino acids (e.g. Asn, Glu, Gln, Ile, Lys, Ser, Tyr and Val) and increases with Pro and Thr. Notably, although the intermediates in both arginine synthesis and degradation pathways were significantly inhibited by the combination across 24 h, the level of arginine itself was not changed differentially. In contrast, both the lysine level and the intermediates related to its biosynthesis and degradation were severely inhibited by the combination during the 24-h period (Fig. 6). Our observation of a dramatic reduction (up to −11.1 $\log_2$FC) in the levels of phosphorylated nucleotides caused by the combination at both time points (e.g. GTP, CTP and UTP; Fig. 6B) is consistent with the increased consumption of these metabolites for phage replication. The substantial reductions in free nucleotide bases (i.e. adenosine, guanosine, cytidine and uridine) at 4 h indicated that phage replication led to rapid nucleotide turnover, which was very likely due to that nucleotide incorporation into the phage genome during replication remarkably exceeded nucleotide biosynthesis by bacterial cells. The greatly increased levels of three cyclic nucleotides (i.e. 2′,3′-cyclic AMP, 3′,5′-cyclic GMP and 2′,3′-cyclic CMP)

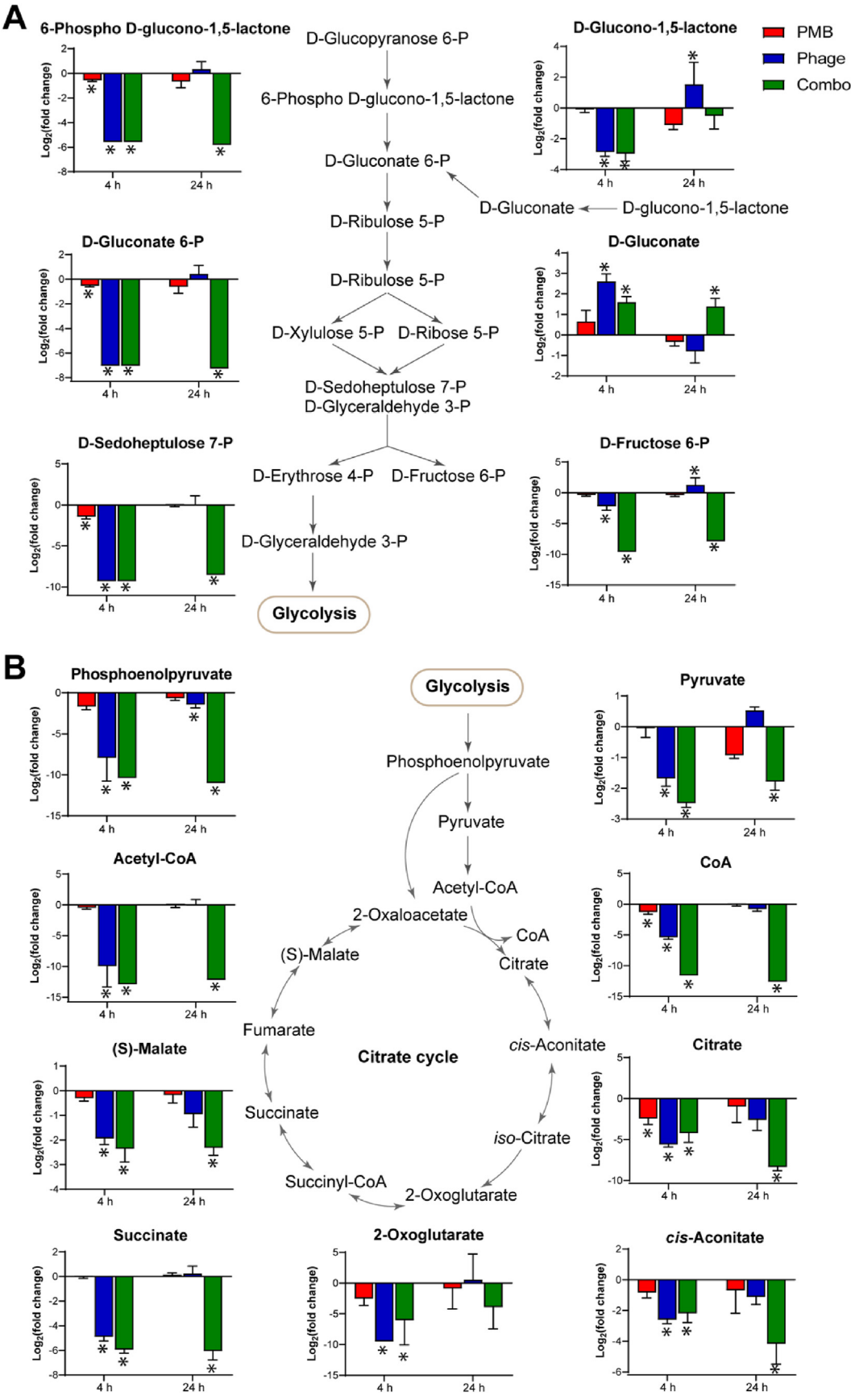


**Fig. 5.** Metabolic changes at 4 and 24 h in the (A) pentose phosphate pathway and (B) citrate cycle in *K. pneumoniae* II-503 following treatments with polymyxin B (PMB) alone, phage pK8 (Phage) alone, and the combination (Combo). The bar charts show $\log_2$FC of metabolite levels compared to the untreated control ($\log_2$FC $\geq 1$ or $\leq -1$, $p$-value <0.05). The asterisks indicated significant metabolic changes compared to the untreated control ($\log_2$FC $\geq 1$ or $\leq -1$, $p$-value <0.05).

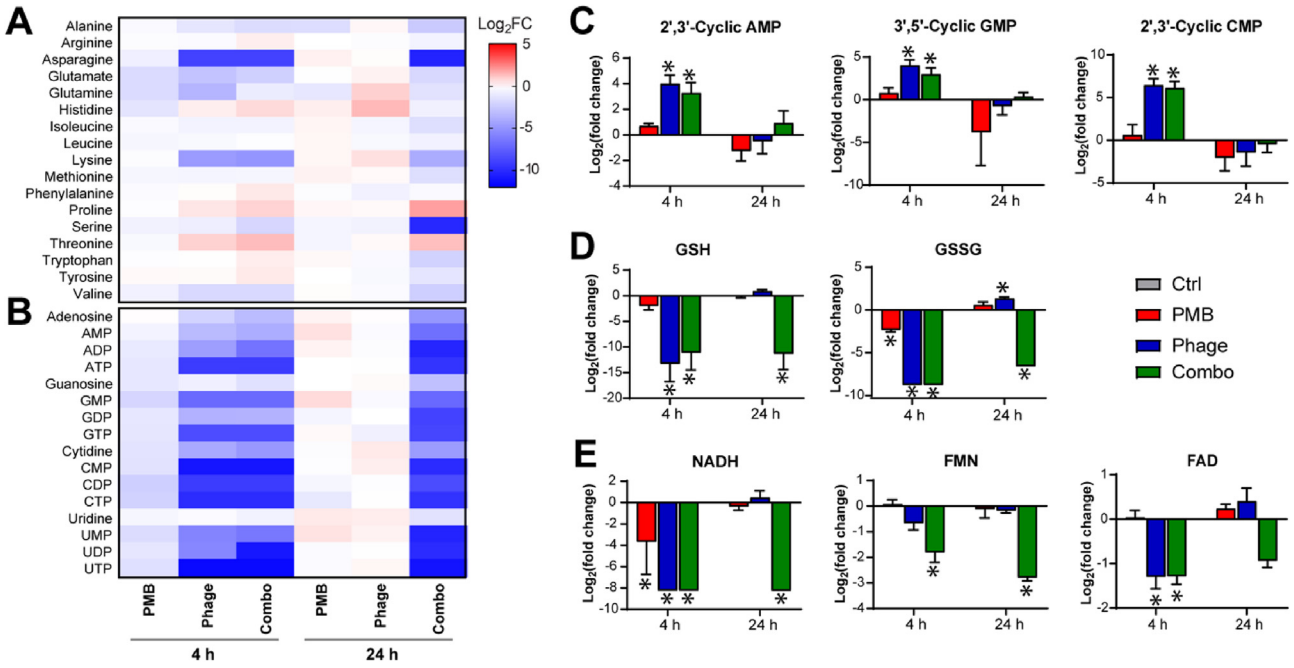


**Fig. 6.** Metabolic changes in amino acids, nucleotides, and related metabolites. Heatmap profiles show metabolic changes in (A) amino acids and (B) nucleotides; Bar charts show the $\log_2$FC of metabolic changes in (C) cyclic nucleotide, (D) glutathione (GSH) and glutathione disulfide (GSSG), and (E) NADH related metabolites. $\text{Log}_2\text{FC} \geq 1$ or $\leq -1$, $p$-value <0.05. Ctrl, control; PMB, polymyxin B; Phage, phage pK8; Combo, the combination. The asterisks indicated significant metabolic changes compared to the untreated control ($\log_2\text{FC} \geq 1$ or $\leq -1$, $p$-value <0.05).

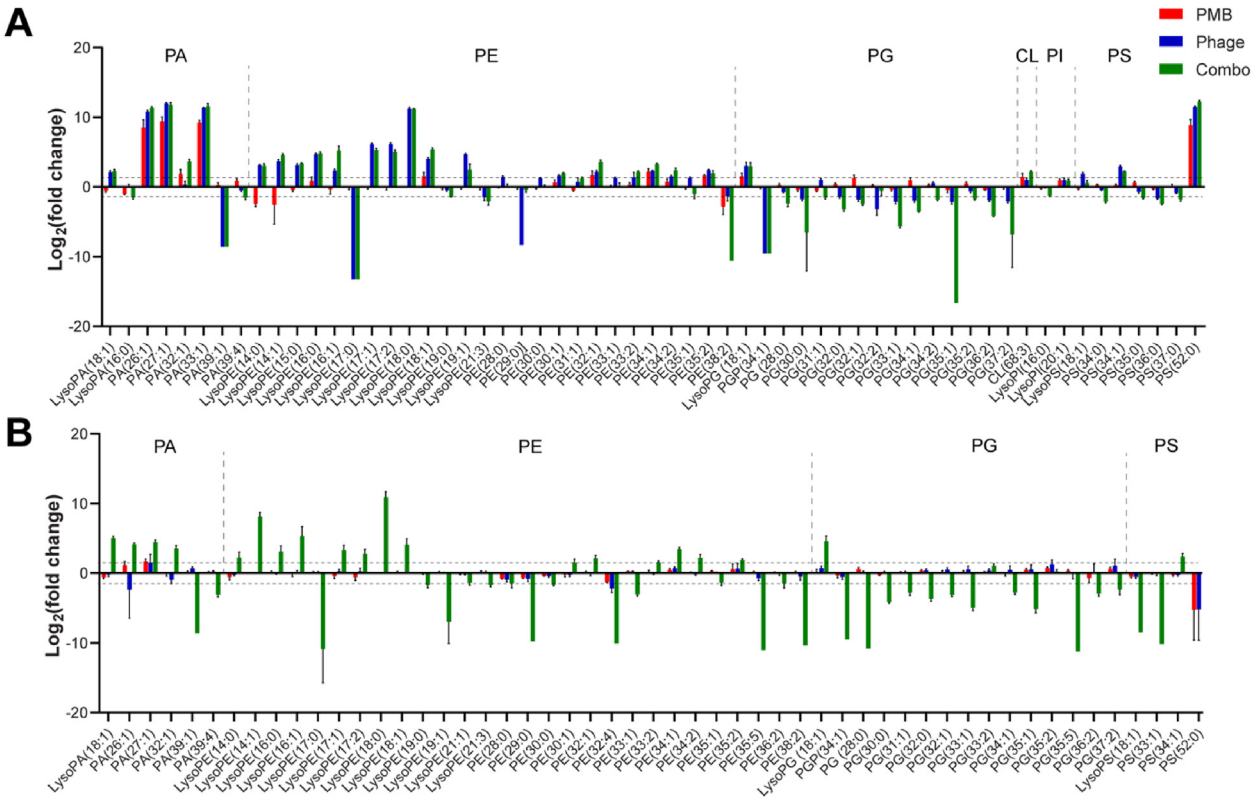


**Fig. 7.** Metabolic changes in different classes of phospholipids in *K. pneumoniae* II-503 following treatment with polymyxin B (PMB) alone, phage pK8 (Phage) alone, and the combination (Combo) compared to the untreated control at (A) 4 h and (B) 24 h. Lipids were putatively annotated based on the accurate mass. PA, phosphatidic acid; PE, phosphatidylethanolamine; PG, phosphatidylglycerol; PI, phosphatidylinositol; PS, phosphatidylserine; and CL, cardiolipin. The horizontal dashed lines represent $\log_2$FC = 1 or −1.

at 4 h also suggested nucleotide turnover while bacteria were experiencing exogenous stress (Fig. 6C) [52]. Overall, our results demonstrated that phage killing significantly affected nucleotide and amino acid metabolism in phage-susceptible bacterial cells, which correlates very well with previous metabolomics studies in *P. aeruginosa* [51,53].

Another important finding of our study is the metabolic changes due to phage treatment, which provide molecular insights into the development of phage resistance [53,54]. Phage-resistant bacteria underwent remodelling in carbon metabolism, particularly the glycolysis pathway (Fig. 4B and 5). Several key precursors in the synthesis of bacterial lipids and the cell wall, D-glyceraldehyde 3-phosphate, D-fructose 6-phoshate and D-sedoheptulose 1,7-biphosphate, were greatly enriched at 24 h following phage monotherapy. In contrast, phosphoenolpyruvate and 3-phospho-D-glycerate, which are essential precursors for amino acid synthesis, were significantly decreased by phage monotherapy and the combination at 24 h. These results suggest that phage replication utilised large amounts of amino acids and thereby depleting these precursors. However, we did not observe a decreased abundance of amino acids with phage alone at 24 h, very likely due to the rapid phage resistance which helped bacterial metabolism return to normal.

Killing of Gram-negative bacteria by polymyxins is initiated by an electrostatic interaction between their positively charged L-α,γ-diaminobutyric acid (Dab) residues and the negatively charged phosphate groups of lipopolysaccharide (LPS) in the outer membrane [25,45,55]. Subsequent membrane disruption results in increased permeability and phospholipid exchange, and eventually cell death [45]. It was not surprising that no substantial bacterial killing was observed with polymyxin B alone (Fig. 1C) given *K. pneumoniae* II-503 contains the plasmid-borne phosphoethanolamine (pEtN) transferase gene *mcr*-1. This gene mediates polymyxin resistance via the addition of pEtN to the lipid A component of LPS in the outer leaflet of the Gram-negative outer membrane [27], decreasing the initial electrostatic interaction with polymyxins. The expression of this gene prevented the severe metabolic perturbations observed in susceptible Gram-negative bacteria treated with polymyxins [32,56], with only the phospholipid levels were affected at 4 h (but not 24 h), consistent with its membrane targeting antimicrobial mechanism. Although no significant bacterial killing was observed with polymyxin B alone at 16 mg/L (Fig. 1C), polymyxin B rapidly depolarised the bacterial membrane potential (e.g. 30 min after treatment) and continued to do so for 24 h (Fig. S2). The polymyxin B-phage combination treatment produced a similar prolonged membrane depolarisation effect. It is most likely that the depolarisation of the outer membrane by polymyxin B plays an important role in the synergistic killing by the combination with phage pK8. Notably, the phage-resistant bacteria detected at 24 h due to phage treatment did not significantly affect polymyxin susceptibility (MIC 8 mg/L), indicating that no cross resistance was generated in *K. pneumoniae*. Further studies are required to elucidate the interplay of bacterial membrane disruption by polymyxin B, bacterial lysis by phage pK8, and the inhibition of bacterial metabolism across 24 h by the polymyxin-phage combination.

## 5. Conclusions

The present study is the first to employ a systems approach to investigate the enhanced bacterial killing by an antibiotic-phage combination against *K. pneumoniae*. The combination of polymyxin B and phage pK8 showed substantially improved antibacterial activity against a polymyxin-resistant *K. pneumoniae* isolate which was dominated by synergistic inhibition of bacterial central carbon, amino acid and nucleotide metabolism. The development of phage resistance was associated with enhanced membrane lipid biosynthesis and decreased amino acid biosynthesis. Our findings provide critical mechanistic information for facilitating the clinical translation of synergistic antibiotic-phage combinations to treat life-threatening multidrug-resistant infections.

## Author contributions

J.L. conceived the project. M.-L.H. performed antimicrobial, metabolomics and SEM experiments, bioinformatic analysis, and wrote the manuscript. S.C.N. conducted DNA sequencing of bacteriophage. Y.W.L. isolated the bacteriophage, H.H.Y. and H.W. performed antimicrobial testing, S.C. performed SEM imaging, and K. C., J.J.B, and R.T.S. contributed to the discussion on phage biology. All authors reviewed the manuscript.

## Declaration of Competing Interest

The authors declare that they have no known competing financial interests or personal relationships that could have appeared to influence the work reported in this paper.

## Acknowledgements

This research was supported by research grants from the National Institute of Allergy and Infectious Disease (NIAID) of the National Institute of Health (R01 AI132154 and R21 AI156766). The content is solely the responsibility of the authors and does not necessarily represent the official views of NIAID. J.L. is an Australian National Health and Medical Research Council (NHMRC) Principal Research Fellow. T.V. and D.J.C. are Australian NHMRC Career Development Research Fellows. The authors would like to thank Monash Proteomics and Metabolomics Facility (Monash University), Monash Micromon Genomics Facility (Monash University), and the Ramaciotti Centre for Cryo-Electron Microscopy (Monash University, the Victorian Node of Microscopy Australia) for providing technical support.

## Appendix A. Supplementary data

Supplementary data to this article can be found online at https://doi.org/10.1016/j.csbj.2021.12.039.

## References

[1] Keynan Y, Rubinstein E. The changing face of *Klebsiella pneumoniae* infections in the community. Int J Antimicrob Agents 2007;30(5):385–9.
[2] Pitout JDD, Nordmann P, Poirel L. Carbapenemase-producing *Klebsiella pneumoniae*, a key pathogen set for global nosocomial dominance. Antimicrob Agents Chemother 2015;59(10):5873–84.
[3] De Oliveira DMP, Forde BM, Kidd TJ, Harris PNA, Schembri MA, Beatson SA, et al. Antimicrobial resistance in ESKAPE pathogens. Clin Microbiol Rev 2020;33(3). https://doi.org/10.1128/CMR.00181-19.
[4] Roberts KD, Azad MAK, Wang J, Horne AS, Thompson PE, Nation RL, et al. Antimicrobial activity and toxicity of the major lipopeptide components of polymyxin B and colistin: last-line antibiotics against multidrug-resistant Gram-negative bacteria. ACS Infect Dis 2015;1(11):568–75.
[5] Abdul Rahim N, Cheah S-E, Johnson MD, et al. Synergistic killing of NDM-producing MDR *Klebsiella pneumoniae* by two 'old'antibiotics—polymyxin B and chloramphenicol. *J Antimicrob Chemother* 2015;70(9):2589–97.
[6] Ah Y-M, Kim A-J, Lee J-Y. Colistin resistance in *Klebsiella pneumoniae*. Int J Antimicrob Agents 2014;44(1):8–15.
[7] Jayol A, Poirel L, Brink A, Villegas M-V, Yilmaz M, Nordmann P. Resistance to colistin associated with a single amino acid change in protein PmrB among *Klebsiella pneumoniae* isolates of worldwide origin. Antimicrob Agents Chemother 2014;58(8):4762–6.
[8] Lee J, Patel G, Huprikar S, Calfee DP, Jenkins SG. Decreased susceptibility to polymyxin B during treatment for carbapenem-resistant *Klebsiella pneumoniae* infection. J Clin Microbiol 2009;47(5):1611–2.

[9] Kortright KE, Chan BK, Koff JL, Turner PE. Phage therapy: a renewed approach to combat antibiotic-resistant bacteria. Cell Host Microbe 2019;25(2):219–32.
[10] Lin DM, Koskella B, Lin HC. Phage therapy: An alternative to antibiotics in the age of multi-drug resistance. World J Gastrointest Pharmacol Therap 2017;8(3):162. https://doi.org/10.4292/wjgpt.v8.i3.162.
[11] Fauconnier A. Phage therapy regulation: from night to dawn. Viruses 2019;11(4):352.
[12] Pelfrene E, Willebrand E, Cavaleiro Sanches A, Sebris Z, Cavaleri M. Bacteriophage therapy: a regulatory perspective. J Antimicrob Chemother 2016;71(8):2071–4.
[13] Loc-Carrillo C, Abedon ST. Pros and cons of phage therapy. Bacteriophage 2011;1(2):111–4.
[14] Pirisi A. Phage therapy—advantages over antibiotics? The Lancet 2000;356(9239):1418.
[15] Tagliaferri TL, Jansen M, Horz H-P. Fighting pathogenic bacteria on two fronts: phages and antibiotics as combined strategy. Front Cell Infect Microbiol 2019;9:22.
[16] Ryan EM, Alkawareek MY, Donnelly RF, Gilmore BF. Synergistic phage-antibiotic combinations for the control of *Escherichia coli* biofilms in vitro. FEMS Immunol Med Microbiol 2012;65(2):395–8.
[17] Knezevic P, Curcin S, Aleksic V, Petrusic M, Vlaski L. Phage-antibiotic synergism: a possible approach to combatting *Pseudomonas aeruginosa*. Res Microbiol 2013;164(1):55–60.
[18] Zhang QG, Buckling A. Phages limit the evolution of bacterial antibiotic resistance in experimental microcosms. Evol Appl 2012;5(6):575–82.
[19] Oechslin F, Piccardi P, Mancini S, et al. Synergistic interaction between phage therapy and antibiotics clears *Pseudomonas aeruginosa* infection in endocarditis and reduces virulence. J Infect Dis 2017;215(5):703–12.
[20] Coulter LB, McLean RJ, Rohde RE, Aron GM. Effect of bacteriophage infection in combination with tobramycin on the emergence of resistance in *Escherichia coli* and *Pseudomonas aeruginosa* biofilms. Viruses 2014;6(10):3778–86.
[21] Ankrah NYD, May AL, Middleton JL, Jones DR, Hadden MK, Gooding JR, et al. Phage infection of an environmentally relevant marine bacterium alters host metabolism and lysate composition. ISME J 2014;8(5):1089–100.
[22] Bedi MS, Verma V, Chhibber S. Amoxicillin and specific bacteriophage can be used together for eradication of biofilm of *Klebsiella pneumoniae* B5055. World J Microbiol Biotechnol 2009;25(7):1145–51.
[23] Chhibber S, Kaur S, Kumari S. Therapeutic potential of bacteriophage in treating *Klebsiella pneumoniae* B5055-mediated lobar pneumonia in mice. J Med Microbiol 2008;57(12):1508–13.
[24] Abedon ST. Phage-antibiotic combination treatments: Antagonistic impacts of antibiotics on the pharmacodynamics of phage therapy? Antibiotics 2019;8(4):182.
[25] Nang SC, Azad MAK, Velkov T, Zhou Q, Li J, Barker E. Rescuing the last-line polymyxins: achievements and challenges. Pharmacol Rev 2021;73(2):679–728.
[26] Zimmerman AE, Howard-Varona C, Needham DM, John SG, Worden AZ, Sullivan MB, et al. Metabolic and biogeochemical consequences of viral infection in aquatic ecosystems. Nat Rev Microbiol 2020;18(1):21–34.
[27] Nang SC, Han M-L, Yu HH, et al. Polymyxin resistance in *Klebsiella pneumoniae*: multifaceted mechanisms utilized in the presence and absence of the plasmid-encoded phosphoethanolamine transferase gene *mcr-1*. *J Antimicrob Chemother* 2019;74(11):3190–98.
[28] Testing ECoAS. Recommendations for MIC determination of colistin (polymyxin E) as recommended by the joint CLSI-EUCAST Polymyxin Breakpoints Working Group. *EUCAST: Växjö, Sweden.* 2016.
[29] Bonilla N, Rojas MI, Netto Flores Cruz G, Hung S-H, Rohwer F, Barr JJ. Phage on tap–a quick and efficient protocol for the preparation of bacteriophage laboratory stocks. PeerJ 2016;4:e2261.
[30] Ács N, Gambino M, Brøndsted L. Bacteriophage enumeration and detection methods. Front Microbiol 2020;11:2662.
[31] Wu G, Yang Q, Long M, Guo L, Li B, Meng Y, et al. Evaluation of agar dilution and broth microdilution methods to determine the disinfectant susceptibility. J Antibiot 2015;68(11):661–5.
[32] Han M-L, Zhu Y, Creek DJ, Lin Y-W, Gutu AD, Hertzog P, et al. Comparative metabolomics and transcriptomics reveal multiple pathways associated with polymyxin killing in *Pseudomonas aeruginosa*. MSystems 2019;4(1). https://doi.org/10.1128/mSystems.00149-18.
[33] Creek DJ, Jankevics A, Burgess KE, Breitling R, Barrett MP. IDEOM: an Excel interface for analysis of LC–MS-based metabolomics data. Bioinformatics 2012;28(7):1048–9.
[34] Smith CA, Want EJ, O'Maille G, Abagyan R, Siuzdak G. XCMS: processing mass spectrometry data for metabolite profiling using nonlinear peak alignment, matching, and identification. Anal Chem 2006;78(3):779–87.
[35] Scheltema RA, Jankevics A, Jansen RC, Swertz MA, Breitling R. PeakML/mzMatch: a file format, Java library, R library, and tool-chain for mass spectrometry data analysis. Anal Chem 2011;83(7):2786–93.
[36] Dunn WB, Erban A, Weber RJM, Creek DJ, Brown M, Breitling R, et al. Mass appeal: metabolite identification in mass spectrometry-focused untargeted metabolomics. Metabolomics 2013;9(S1):44–66.
[37] Chong J, Soufan O, Li C, et al. MetaboAnalyst 4.0: towards more transparent and integrative metabolomics analysis. *Nucleic Acids Res.* 2018;46(W1):W486-W494.
[38] Noble WS. How does multiple testing correction work? Nat Biotechnol 2009;27(12):1135–7.
[39] Zheng W, Sun W, Simeonov A. Drug repurposing screens and synergistic drug-combinations for infectious diseases. Br J Pharmacol 2018;175(2):181–91.
[40] Kaye KS, Pogue JM, Tran TB, Nation RL, Li J. Agents of last resort: polymyxin resistance. Infect Dis Clin North Am 2016;30(2):391–414.
[41] van de Putte P, Cramer S, Giphart-Gassler M. Invertible DNA determines host specificity of bacteriophage Mu. Nature 1980;286(5770):218–22.
[42] North OI, Sakai K, Yamashita E, Nakagawa A, Iwazaki T, Büttner CR, et al. Phage tail fibre assembly proteins employ a modular structure to drive the correct folding of diverse fibres. Nat Microbiol 2019;4(10):1645–53.
[43] Poudyal A, Howden BP, Bell JM, Gao W, Owen RJ, Turnidge JD, et al. In vitro pharmacodynamics of colistin against multidrug-resistant *Klebsiella pneumoniae*. J Antimicrob Chemother 2008;62(6):1311–8.
[44] Catalão MJ, Gil F, Moniz-Pereira J, São-José C, Pimentel M. Diversity in bacterial lysis systems: bacteriophages show the way. FEMS Microbiol Rev 2013;37(4):554–71.
[45] Velkov T, Roberts KD, Nation RL, Thompson PE, Li J. Pharmacology of polymyxins: new insights into an 'old' class of antibiotics. Fut Microbiol 2013;8(6):711–24.
[46] Manning AJ, Kuehn MJ. Contribution of bacterial outer membrane vesicles to innate bacterial defense. BMC Microbiol 2011;11(1):258. https://doi.org/10.1186/1471-2180-11-258.
[47] MacDonald IA, Kuehn MJ. Stress-induced outer membrane vesicle production by *Pseudomonas aeruginosa*. J Bacteriol 2013;195(13):2971–81.
[48] Eisenreich W, Dandekar T, Heesemann J, Goebel W. Carbon metabolism of intracellular bacterial pathogens and possible links to virulence. Nat Rev Microbiol 2010;8(6):401–12.
[49] Noor E, Eden E, Milo R, Alon U. Central carbon metabolism as a minimal biochemical walk between precursors for biomass and energy. Mol Cell 2010;39(5):809–20.
[50] Altamirano FLG, Barr JJ. Phage therapy in the postantibiotic era. Clin Microbiol Rev 2019;32(2):e00066–00018.
[51] Chevallereau A, Blasdel BG, De Smet J, Monot M, Zimmermann M, Kogadeeva M, et al. Next-generation "-omics" approaches reveal a massive alteration of host RNA metabolism during bacteriophage infection of *Pseudomonas aeruginosa*. PLoS Genet 2016;12(7):e1006134.
[52] Botsford JL. Cyclic nucleotides in procaryotes. Microbiol Rev 1981;45(4):620–42.
[53] De Smet J, Zimmermann M, Kogadeeva M, Ceyssens P-J, Vermaelen W, Blasdel B, et al. High coverage metabolomics analysis reveals phage-specific alterations to *Pseudomonas aeruginosa* physiology during infection. ISME J 2016;10(8):1823–35.
[54] Labrie SJ, Samson JE, Moineau S. Bacteriophage resistance mechanisms. Nat Rev Microbiol 2010;8(5):317–27.
[55] Velkov T, Thompson PE, Nation RL, Li J. Structure– activity relationships of polymyxin antibiotics. J Med Chem 2010;53(5):1898–916.
[56] Maifiah MHM, Creek DJ, Nation RL, Forrest A, Tsuji BT, Velkov T, et al. Untargeted metabolomics analysis reveals key pathways responsible for the synergistic killing of colistin and doripenem combination against *Acinetobacter baumannii*. Sci Rep 2017;7(1). https://doi.org/10.1038/srep45527.